Composites & nanocomposites

The suitability of common reed (*Phragmites australis*) for load-bearing structural materials

Kaspar Albrecht[1], Felix Neudecker[1], Stefan Veigel[1], Sabine Bodner[2], Jozef Keckes[2], and Wolfgang Gindl-Altmutter[1,*] (ID)

[1] *Department of Materials Science and Process Engineering, BOKU – University of Natural Resources and Life Science, Vienna, Konrad Lorenz Strasse 24, 3430 Tulln, Austria*

[2] *Chair of Materials Physics, Montanuniversität Leoben, Jahnstrasse 12/I, 8700 Leoben, Austria*

ABSTRACT

Besides wood, the most widely used natural structural material, dicotyledonous fibre plants such as flax or hemp, and monocotyledonous grasses such as cereal straw or bamboo have been shown to be suitable for application in materials. Common reed is a less well-characterised plant resource in this regard. Therefore, common reed stems were characterised in uniaxial tension in the present study, aiming at acquiring basic information about the mechanical characteristics of this material. Furthermore, laboratory-scale composite beams were manufactured and tested in bending. Compared to wood species with similar density, common reed stem walls showed a comparable average modulus of elasticity of 8 GPa and a very good average tensile strength of 150 MPa. After a mild alkali pretreatment, reed showed excellent adhesive bonding, enabling the manufacture of high-density composite beams with roughly 130 MPa bending strength and 12–13 GPa modulus of elasticity. Same as untreated common reed stem walls, also reed biocomposite beams compared very favourably with established wood-based materials of similar structure, density, and adhesive content. In summary, it was thus demonstrated that common reed is a highly suitable raw material for bio-based load-bearing structural materials.

Introduction

Recently, there has been a rapidly growing interest in substituting fossil-based structural materials with renewable or renewable-based alternatives [1–3]. Renewable materials, particularly wood-based products, perform exceptionally well mechanically, and notably also in terms of reducing carbon emissions in construction [2]. Besides forest-based resources, i.e. timber, also natural fibres [4, 5], bamboo [6, 7], cereal straw [8, 9] and other plant fibres are considered potential sustainable raw materials. One source of biomass that shows so far little exploited potential to substitute fossil-based materials is *Phragmites Australis,* from

---

https://doi.org/10.1007/s10853-023-08996-1

Springer

this point onwards referred to as "common reed" or "reed". Common reed is an undemanding and highly productive aquatic grass widely available worldwide due to its invasive spread [10]. In Europe, reed is one of the most abundant aquatic plants and embodies a major element of the lake flora [11–13]. In fact, the management of reed by mowing during winter benefits lake ecosystems [14]. Historically, reed was used for roof thatching, flooring, wind protection, and as fodder plant, if not burned directly on site in the worst case. More recently, the use of reed in bio-based thermal insulation [15–17], and in biorefinery approaches towards biotechnological valorisation have been discussed [18–20].

Branchless stems of reed, which grow vertically and straight upwards and show a cylindrical, hollow structure, can reach a height of up to 5 m and a diameter of up to 15 mm. At the top of the reed stems, panicles that usually contain 2–10 spikelets are found. The deciduous leaves, which are wide at the lower part and sharpened on the top, grow out of the leaf sheaths [11].

The walls of the hollow reed stem are typically less than 1 mm thick. As shown in Fig. 1a thick-walled sclerenchyma and epidermis are concentrated in the outermost wall regions, contributing optimally to the strength and stiffness of the stem [21], and a waxy layer forms the outermost barrier. Straight and structurally homogeneous internodes with a length

between roughly 20–30 cm are joined together in the nodes (Fig. 1b), where the structures of consecutive internodes merge, showing significant structural heterogeneity compared to internodes. The chemical composition of reed stems (Table 1) is similar to other lignocellulosic resources, with the exception of a high content in extractives and inorganic compounds [19, 20, 22–25]. Among the latter, high silicon content is typical of reed [26]. Both the silicon content and the content of lipophilic extractives need to be significantly reduced in order to enhance adhesion in reed composite processing [27–29].

A limited number of studies have already dealt with the conversion of reed into chemicals through biorefineries [30] and into structural materials. In the latter publications, small particles or fibres of reed prepared by grinding or milling were used as raw material and densified afterwards. Following pre-treatment with 2% NaOH solution, a binderless reed fibre board was produced [29], which showed a modulus of elasticity of 2.5 GPa. Also using reed fibres, urea-formaldehyde resin bonded medium density fibre board [27] and formaldehyde-free particleboard [31] were produced, and

Table 1 Range of chemical composition of reeds from different sources [19, 20, 22–25] as mean values in % of dry matter

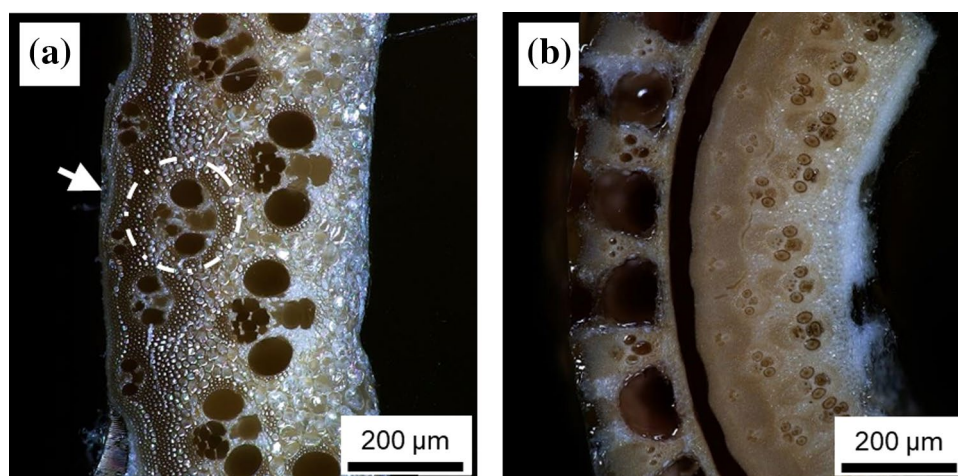| Cellulose (%)	Hemicellulose (%)	Lignin (%)	Others (%)
33–51	20–28	10–24	10–22

Figure 1 Cross section through the wall of a reed stem showing. **a** Intermodal region with the waxy layer at the outermost surface (arrow), the epidermis and a dense layer of sclerenchyma with thick cell walls, followed by less dense tissue containing numerous vascular bundles (one representative bundle is indicated by a circle). **b** cross section through a stem in the nodal region connecting two internodes.

the properties of reed fibres as filler for high-density polyethylene composites were discussed [32, 33]. Some isolated data indicate appreciable tensile strength of 96–112 MPa for reed stems [34, 35], but studies explicitly focussing on the feasibility of high-performance reed-based materials for structural applications were not found by the authors. Therefore, the present study aims at a thorough characterisation of the tensile properties of reed stems and, in a second step, at assessing the feasibility of unidirectional model composites with high strength.

Materials and methods

Common reed

Reed stems with a length of 100–150 cm and diameters of 3–8 mm, respectively, were harvested from a wet meadow next to Konrad Lorenz Strasse 24 in 3430 Tulln, Austria, from March to May 2022 and peeled off leaves. Prior to further processing the stems with an as-harvested moisture content between 8 and 35% were equilibrated in a climate chamber kept at 20 °C and 65% relative humidity.

Characterisation of reed stems

For light microscopy, specimens 10 mm long and 3 mm wide were embedded in low viscosity epoxy resin (Agar Scientific) under vacuum. Smooth cuts through the cross section of the specimens were subsequently obtained using a microtome (Leica Ultracut R) equipped with a diamond knife (Diatome T-735 trim 45). All light microscopy was performed using a digital light microscope (Olympus DSX1000).

Soxhlet extraction was carried out to determine the content of nonpolar substances present in reed stems. Stems were cut into pieces of 2 cm length and then milled with an ultra-centrifugal mill (Retsch ZM 200) with a 1-mm sieve insert. Extraction was carried out with n-hexane (CAS 110-54-3, Carl Roth GmbH+Co. KG) for five hours. The content of solubles was determined gravimetrically after solvent evaporation (Heidolph Laborota 400).

Thermogravimetric analysis (TGA Netzsch TG 209 F1) was carried out with milled reed stems using the fraction passing a 0.5-mm sieve. Approximately 10 mg of material was placed in a 85 μL Al_2O_3 crucibles and covered with a punched lid. Analyses were performed

between 25 and 800 °C at a heating rate of 20 °C min^{-1} and a constant air flow of 40 mL min^{-1}, respectively.

The tensile strength of reed stems was characterised using a universal testing machine (Zwick/Roell Z100). Specimens were prepared with a length of 100 mm and a width of 2–3 mm. Birch wood veneer patches were glued to the ends of the specimens in order to provide an appropriate gripping area, resulting in a free length of 50 mm which was actually tested. Twelve specimens per variant were characterised at a testing speed of 1 mm min^{-1}. Prior to testing, the density of each specimen was determined gravimetrically.

Wide-angle X-ray scattering (WAXS) of a thin slice of internodal material was carried out using a Nanostar (Bruker AXS). The device included an Incoatec Microfocus source supplying Cu-Kα rays, two-pinhole collimation system, 2D Montel optics and a 2D Image Plate detector. For the further processing of the data, the software Fit2D was used. The intensity distribution of 2D detector images was quantified, and the azimuthal variation of intensity along the cellulose I (200) reflection was evaluated. The resulting intensity distribution curve I(ϕ) was fitted with a Gaussian, which was then used to calculate the orientation factor $\sin^2\phi$ according to the following Eq. (1):

$$\sin^2\phi = \frac{\int_0^{\frac{\pi}{2}} I(\phi)\sin^3\phi\,\mathrm{d}\phi}{\int_0^{\frac{\pi}{2}} I(\phi)\sin\phi\,\mathrm{d}\phi} \tag{1}$$

Composite preparation and characterisation

In order to study the feasibility of composite materials based on reed, small beams consisting of parallel aligned stems containing both internodal sections and nodes bonded with wood adhesive were produced. For wheat straw, it is known that a waxy surface layer strongly impedes efficient adhesive bonding [36]. Therefore, preliminary tests were carried out using untreated reed stem slices in combination with a commercial phenol-resorcinol-formaldehyde resin (PRF, Aerodux 185, Metadynea Austria GmbH) and a one-component polyurethane adhesive (PUR, Loctite HB S309, Henkel AG & Co. KG). Also, it was decided to include a mild alkaline pre-treatment step prior to composite manufacture for a part of the specimens to be produced. Since it was reported elsewhere that already pre-treatment at 1% NaOH led to noticeable loss of lignin and hemicellulose [25],

the concentration for this pre-treatment was set to 0.4% (0.1 Mol L^{-1}) NaOH. Longitudinal slices of reed with a length of 300 mm and 2–5 mm in width were prepared. The variant subject to alkali pre-treatment was submerged in 0.1 Mol L^{-1} NaOH at 60 °C for 30 min. Thereafter, the material was washed with deionised water until the washing water reached pH 7. All specimens, whether pre-treated or not (Table 2), were again equilibrated at 20 °C and 65% relative humidity before further processing.

After the application of adhesive with a roller, aligned strands were placed in a steel mould coated with release agent and pressed in a heated hydraulic pressing machine (Langzauner GmbH; Lambrecht, Austria), resulting in composite specimens 300 mm long, 20 mm wide and approx. 3–5 mm thick. From these beams, specimens with 120 mm and 90 mm length were cut for three-point bending and impact bending, respectively. The effective adhesive content of the composite beams was determined from the difference between their final mass in equilibrated condition with their mass prior to adhesive application. It was decided to produce a PUR-bonded composite also with untreated reed because it is known that PUR is more capable of developing sufficient adhesion with surfaces of reduced polarity compared to PRF [37].

The mechanical properties of the composite beams were evaluated in three-point bending using a universal testing machine (Zwick/Roell Z020). Five specimens were tested for each variant, using a test speed of 1 mm min^{-1} at a span width of 70 mm. Furthermore, impact toughness was measured with a pendulum impact tester (Zwick/Roell HIT 50P) equipped with a 5-Joule pendulum.

Table 2 Variants of composite beam specimens produced

| Adhesive	Pre-treatment	Pressing		
		Time (min)	Temperature (min)	Pressure (MPa)
PUR	none	100	25	8.3
PUR	0.1 Mol/L NaOH	100	25	8.3
PRF	0.1 Mol/L NaOH	45	80	8.3

Results and discussion

Untreated reed stems

For mechanical testing, specimens were taken from the lower, middle, and upper third of the plant height, respectively. Furthermore, also specimens containing nodes were considered. As shown in Fig. 1, the structure of the nodal region greatly differs from the internodal sections, which is why different mechanical strength was expected for the latter, as has already been described for wheat straw [38]. The results of tensile tests are shown in Fig. 2. Overall, the level of strength and elasticity observed for internodal specimens, which dominate the reed stem with a length fraction of > 95% of the total stem length, is impressive. For all internodes tested, an average tensile strength of 150 ± 35 MPa and an elastic modulus of 8.1 ± 1.6 GPa were observed. The only known comparable study dealing with reed, to the best knowledge of the authors, reports a tensile strength value of 112 MPa at a density of 0.54 g cm^{-3}[34]. With density ranging from 0.3 to 0.5 g cm^{-3} observed for reed in the present study, low- to moderate-density wood may serve as an appropriate reference. While woods of this density characteristically show similar modulus of elasticity, their tensile strength hardly exceeds 100 MPa [39]. In clear contrast, reed internodes tested in the present study regularly exceed this threshold with individual values even reaching 200 MPa strength. Also compared to chemically and structurally more similar wheat straw internodes, with average tensile strength of 66 MPa [38], reed shows excellent performance. The overall mechanical potential of reed stems is, however, diminished by the comparably poor performance of nodal regions. Here, elastic modulus was reduced to a third of the values observed for internodes, while tensile strength diminished even more significantly (Fig. 2d). Again, even nodal regions of reed, with an overall average of 60 ± 13 MPa, showed better strength than corresponding wheat straw specimens (12.4 MPa) [38].

The fact that the mechanical performance of reed stems is comparable with wood of similar density is in good accordance with the chemical composition of this material (Table 1), which is well comparable with wood. Furthermore, X-ray characterisation revealed that also the degree of preferred orientation of cellulose, which is crucial for good mechanics [40], is in a very similar range as is observed for spruce

Figure 2 Density, tensile strength, and elastic modulus of untreated reed stem specimens from internodes (**a**, **c**) and nodes (**b**, **d**) tested in tension.
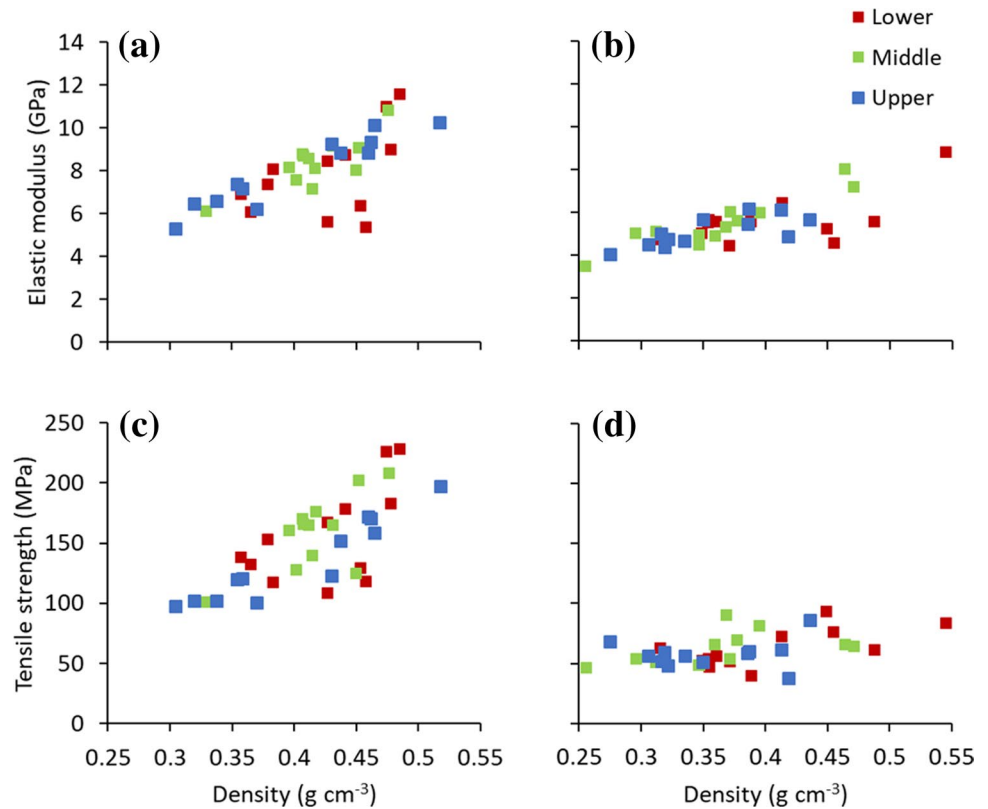
wood. Figure 3 shows a WAXS detector image from the intermodal region of a reed stem. Various scattering peaks typical of the cellulose I crystal are present, where the most intense peak is related to the cellulose I (200) crystalline plane [41]. An inset in Fig. 3 shows a representative WAXS pattern of spruce wood which, upon visual inspection, shows great similarity with the WAXS pattern of reed. The azimuthal cellulose I (200) scattering intensity distribution for reed is also shown in an inset in Fig. 3. Here, distinct and narrow peaks of intensity indicate a high degree of preferred orientation of cellulose crystals parallel to the axis of the reed stem. Numerical integration of this intensity distribution according to Eq. (1) resulted in an orientation factor $\sin^2\phi = 0.092$ for the reed stem material. This value is well comparable with $\sin^2\phi = 0.087$ determined for a representative specimen of spruce wood by the authors, confirming high cellulose orientation for reed.

Composite reed beams

Preliminary trials with PRF adhesive and untreated reed revealed insufficient adhesion strength. While the PRF resin used is generally very efficient in adhesive
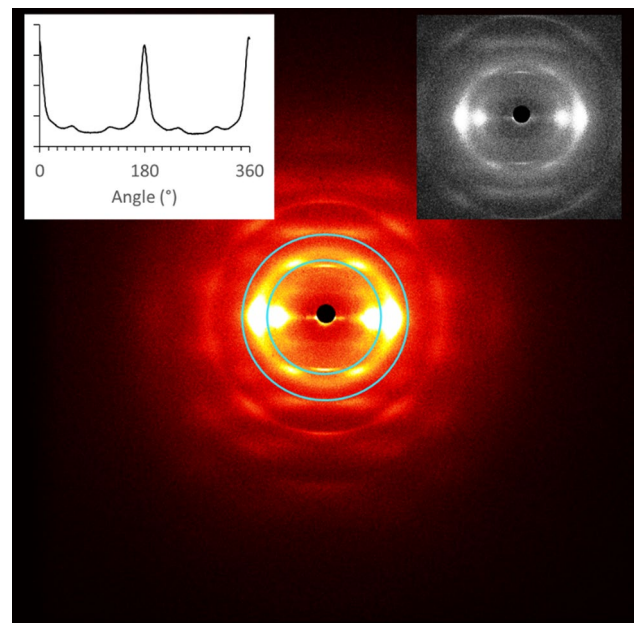

Figure 3 Wide-angle X-ray scattering pattern of a slice of a common reed stem, together with the azimuthal intensity distribution along the most intense cellulose I (200) reflection (top left). Furthermore, the figure shows a representative scattering pattern of spruce wood for reference (top right).

bonding of a broad variety of wood composites, unsatisfying adhesive bonds prone to delamination were obvious as shown in Fig. 4.

Contrarily, preliminary tests with PUR showed good apparent adhesion. Since difficulties with adhesive bonding were expected after preliminary trials with phenolic resin (Fig. 4), the amount of nonpolar substances present in reed biomass was evaluated at first. Using *n*-hexane solvent, gravimetrical determination revealed 1.0% mass of nonpolar extractives. Having ascertained the presence of nonpolar substances and keeping in mind the results of preliminary adhesive bonding tests, it was decided to subject reed biomass to a mild alkaline treatment with 0.1 Mol L^{-1} NaOH in order to improve adhesion. As a result, considerable mass loss occurred, which resulted in a 19.1% reduction of reed stem wall density. Notwithstanding this reduction in density, the mechanical performance of reed stem walls even increased by 10% for tensile strength and 16% for the modulus of elasticity, respectively. Thermogravimetric analysis of the untreated and alkaline-treated variants, however, did not reveal clear differences as shown in Fig. 5. It is thus concluded that the mild pre-treatment conditions chosen herein did not significantly affect the composition of reed cell wall polymers. Compared to the reference, treated reed showed a slightly earlier onset of degradation (261.6 °C instead of 264.6 °C) and a reduced ash content (1.16% instead of 2.52%). The latter may be attributed to the dissolution of silica by the NaOH solution, since the solubility of silica is known to increase sharply at rising pH value [42].

Reed biocomposite specimens produced from treated and untreated reed are shown in Fig. 6. While the untreated PUR variant largely retained the natural appearance of the raw reed stems with a light brown
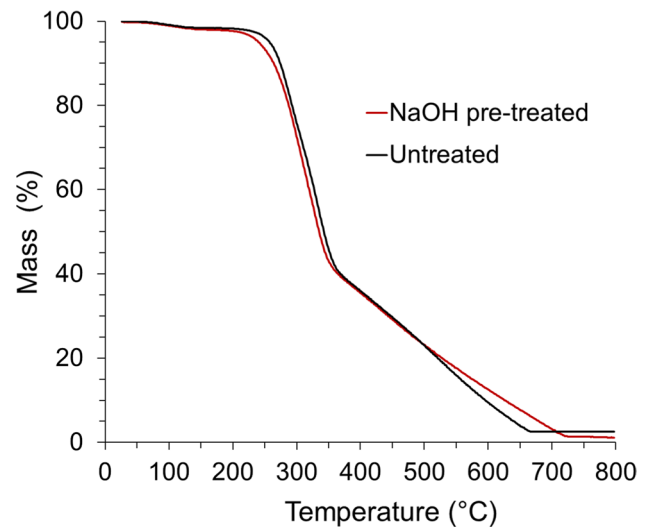

Figure 5 Thermogravimetry of untreated and alkaline-treated reed stem walls.

shade, the pre-treated PUR variant appeared somewhat darker. The pre-treated PRF variant showed a non-uniform dark and red-brown coloration depending on the distribution of dark PRF resin on the reed surface.

The adhesive content of the reed biocomposites differed significantly between the three variants produced (Fig. 7). With on average 15.5% the lowest adhesive content was measured for the alkali pre-treated and PRF-bonded biocomposites, followed by the alkali pre-treated PUR biocomposites (16.5%) and untreated PUR biocomposites (20.7%). The trend

Figure 4 Spontaneous delamination of untreated reed stems bonded with phenol-resorcinol–formaldehyde resin after pressing.

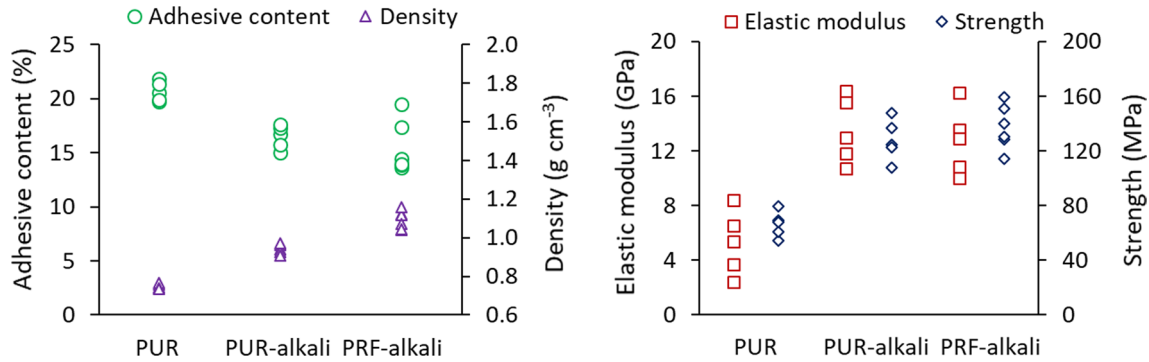**Figure 6** Optical appearance of different reed biocomposite beam specimens.

Figure 7 Adhesive content and density as well as the elastic modulus and strength measured in three-point bending for three variants of reed biocomposite beams.
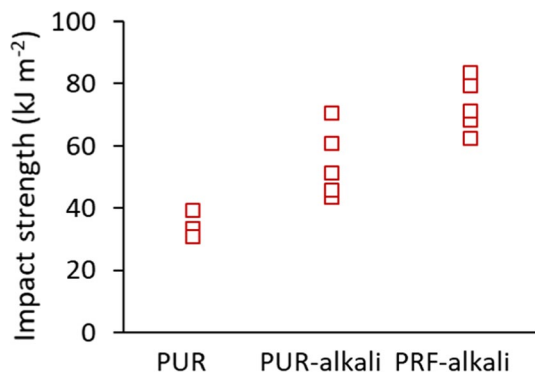

Figure 8 Impact performance of three different variants of reed biocomposite beams.

of variability in adhesive content corresponds well to differences observed in specimen density (Fig. 7), where the untreated PUR variant is lowest and the PRF variant is highest. Some part of the observed differences in density may be explained by the fact that alkali treatment led to an increase in reed density by roughly 20%, enabling higher densification in beams composed of treated reed. The trend towards higher density and lower adhesive content (i.e. higher fibre content) in alkali-treated reed composites results in clearly improved mechanical performance for the latter (Figs. 7, 8). The PUR-bonded composite made from untreated reed shows only modest performance with on average 66 MPa bending strength and 5.2 GPa modulus of elasticity. By contrast, with roughly 130 MPa bending strength and 12–13 GPa modulus of elasticity the composite beams made from alkali-treated reed show excellent performance, regardless of the type of adhesive used. A comparison of the failure mode of untreated specimens, which failed by delamination due to shear forces and treated specimens, which

failed in the tensile zone of the bending specimens, indicates that lack of adhesion limits the performance of composites made with untreated reed stems. Impact performance, as shown in Fig. 8, agrees with this observation. The clearly better mechanical performance of alkali-treated composites indicates that the applied pre-treatment effectively removed the waxy layer of the stem. For untreated reed stems, this layer seems to highly impede wetting by the adhesive, ultimately resulting in poor adhesion and composite strength.

While solid wood is already cited as an appropriate reference material for an appraisal of the mechanical performance of untreated reed stems, several wood-based composite materials are available as benchmarks for reed biocomposite beams. Typically, these unidirectional wood composites consist of elongated wood strands or macro-fibres and 15–30% adhesive [39]. As shown in Fig. 9, reed biocomposite beams are well within the performance range of selected unidirectional wood composites, even when the lower density of the wood-based materials is taken into account.

Conclusion

In summary, this work provides a holistic characterisation of the stems of common reed. The wetland plant shows high potential in availability, and its stems serve as a sustainable source of biomass with high-strength properties due to their high cellulose content. As the trend to replace fossil-based materials with bio-based alternatives intensifies, reed presumably will become increasingly attractive as a biomass resource for materials in the future. Thus, further research is required to
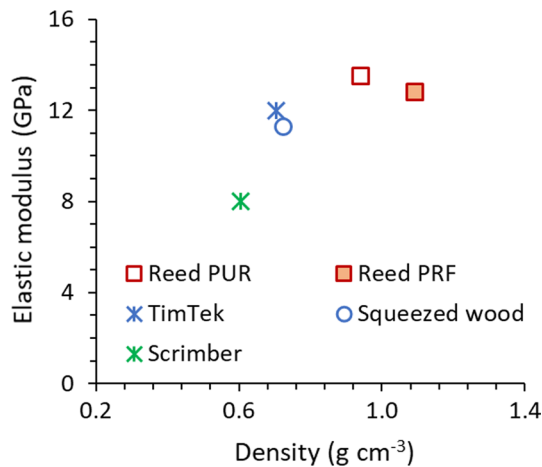
Figure 9 Density and elastic modulus of unidirectional wood composite materials compared to reed biocomposites. Data for TimTek, scrimber and squeezed wood from ref [43].

establish promising process technologies and harvesting schemes to ensure efficient utilisation providing valuable products.

Acknowledgements

Author contributions

Not applicable.

Funding

Data availability

Data will be made available upon request.

Declarations

Conflict of interest The authors are not aware of any conflicts of interest.

Ethical approval Not applicable.

References

[1] Ramage MH, Burridge H, Busse-Wicher M, Fereday G, Reynolds T, Shah DU, Wu G, Yu L, Fleming P, Densley-Tingley D, Allwood J, Dupree P, Linden PF, Scherman O (2017) The wood from the trees: the use of timber in construction. Renew Sustain Energy Rev 68:333–359. https://doi.org/10.1016/j.rser.2016.09.107

[2] Mishra A, Humpenöder F, Churkina G, Reyer CPO, Beier F, Bodirsky BL, Schellnhuber HJ, Lotze-Campen H, Popp A (2022) Land use change and carbon emissions of a transformation to timber cities. Nat Commun 13:4889. https://doi.org/10.1038/s41467-022-32244-w

[3] Orhon AV, Altin M (2020) Utilization of alternative building materials for sustainable construction. In: Dincer I, Colpan CO, Ezan MA (eds) Environmentally-benign energy solutions. Springer, Cham, pp 727–750. https://doi.org/10.1007/978-3-030-20637-6_36

[4] Bourmaud A, Beaugrand J, Shah DU, Placet V, Baley C (2018) Towards the design of high-performance plant fibre composites. Prog Mater Sci 97:347–408. https://doi.org/10.1016/j.pmatsci.2018.05.005

[5] Shah DU (2013) Developing plant fibre composites for structural applications by optimising composite parameters: a critical review. J Mater Sci 48:6083–6107. https://doi.org/10.1007/s10853-013-7458-7

[6] Li Z, Chen C, Mi R, Gan W, Dai J, Jiao M, Xie H, Yao Y, Xiao S, Hu L (2020) A strong, tough, and scalable

structural material from fast-growing bamboo. Adv Mater 32:1906308. https://doi.org/10.1002/adma.201906308

[7] Sharma B, Gatóo A, Bock M, Ramage M (2015) Engineered bamboo for structural applications. Constr Build Mater 81:66–73. https://doi.org/10.1016/j.conbuildmat.2015.01.077

[8] Chougan M, Ghaffar SH, Al-Kheetan MJ, Gecevicius M (2020) Wheat straw pre-treatments using eco-friendly strategies for enhancing the tensile properties of bio-based polylactic acid composites. Ind Crops Prod 155:112836. https://doi.org/10.1016/j.indcrop.2020.112836

[9] Neudecker F, Jakob M, Bodner SC, Keckes J, Buerstmayr H, Gindl-Altmutter W (2023) Delignification and densification as a route to enable the use of wheat straw for structural materials. ACS Sustain Chem Eng 11:7596–7604. https://doi.org/10.1021/acssuschemeng.3c01375

[10] El-Ramady HR, Abdalla N, Alshaal T, Fári M, Prokisch J, Pilon-Smits EAH, Domokos-Szabolcsy É (2015) Selenium phytoremediation by Giant Reed. In: Lichtfouse E, Schwarzbauer J, Robert D (eds) Hydrogen production and remediation of carbon and pollutants. Springer, Cham, pp 133–198. https://doi.org/10.1007/978-3-319-19375-5_4

[11] Rodewald-Rudescu L (1974) Das Schilfrohr. Phragmites communis Trinius. Die Binnengewasser Band 27. E. Schweizerbart'sche, Stuttgart, ix + 302 p. + 11 plates. DM97.50. Limnol Oceanogr 20:1059–1059. https://doi.org/10.4319/lo.1975.20.6.1059a

[12] Csaplovics E (2019) Der Schilfgürtel des Neusiedler Sees. Oesterr Wasser Abfallwirtsch 71(11):494–507. https://doi.org/10.1007/s00506-019-00622-2

[13] Srivastava J, Kalra SJS, Naraian R (2014) Environmental perspectives of *Phragmites australis* (Cav.) Trin. Ex Steudel. Appl Water Sci 4:193–202. https://doi.org/10.1007/s13201-013-0142-x

[14] Ostendorp W, Iseli C, Krauss M, Krumscheid-Plankert P, Moret J-L, Rollier M, Schanz F (1995) Lake shore deterioration, reed management and bank restoration in some Central European lakes. Ecol Eng 5:51–75. https://doi.org/10.1016/0925-8574(95)00014-A

[15] Malheiro R, Ansolin A, Guarnier C, Fernandes J, Amorim MT, Silva SM, Mateus R (2021) The potential of the reed as a regenerative building material—characterisation of its durability, physical, and thermal performances. Energies 14(14):4276. https://doi.org/10.3390/en14144276

[16] Bakatovich A, Gaspar F, Boltrushevich N (2022) Thermal insulation material based on reed and straw fibres bonded with sodium silicate and rosin. Constr Build Mater 352:129055. https://doi.org/10.1016/j.conbuildmat.2022.129055

[17] Karademir A, Yetis F, Imamoglu S, Varlıbas H (2013) Utilization of water reed in production of various insulation panels. Sci Eng Compos Mater 20:371–377. https://doi.org/10.1515/secm-2013-0014

[18] Shuai W, Chen N, Li B, Zhou D, Gao J (2016) Life cycle assessment of common reed (*Phragmites australis* (Cav) Trin. ex Steud) cellulosic bioethanol in Jiangsu Province, China. Biomass Bioenergy 92:40–47. https://doi.org/10.1016/j.biombioe.2016.06.002

[19] Cotana F, Cavalaglio G, Pisello AL, Gelosia M, Ingles D, Pompili E (2015) Sustainable ethanol production from common Reed (*Phragmites australis*) through simultaneuos saccharification and fermentation. Sustainability 7:12149–12163. https://doi.org/10.3390/su70912149

[20] Szijártó N, Kádár Z, Varga E, Thomsen AB, Costa-Ferreira M, Réczey K (2009) Pretreatment of Reed by wet oxidation and subsequent utilization of the pretreated fibers for ethanol production. Appl Biochem Biotechnol 155:83–93. https://doi.org/10.1007/s12010-009-8549-4

[21] Wang X, Deng Y, Wang S, Liao C, Meng Y, Pham T (2013) Nanoscale characterization of reed stalk fiber cell walls. BioResources 8(2):1986–1996. https://doi.org/10.15376/biores.8.2.1986-1996

[22] Scherzinger M, Kaltschmitt M, Thoma M (2021) Effects of vapothermal pretreatment on anaerobic degradability of common Reed. Energy Technol 9:2001046. https://doi.org/10.1002/ente.202001046

[23] Arufe S, Hellouin de Menibus A, Leblanc N, Lenormand H (2021) Physico-chemical characterisation of plant particles with potential to produce biobased building materials. Ind Crops Prod 171:113901. https://doi.org/10.1016/j.indcrop.2021.113901

[24] Başaran Kankılıç G, Metin AÜ (2020) Phragmites australis as a new cellulose source: extraction, characterization and adsorption of methylene blue. J Mol Liquids 312:113313. https://doi.org/10.1016/j.molliq.2020.113313

[25] Pandiarajan P, Kathiresan M (2018) Physicochemical and mechanical properties of a novel fiber extracted from the stem of common reed plant. Int J Polym Anal Charact 23(5):442–449. https://doi.org/10.1080/1023666X.2018.1474327

[26] Wöhler-Geske A, Moschner CR, Gellerich A, Militz H, Greef JM, Hartung E (2016) Provenances and properties of thatching reed (*Phragmites australis*). Appl Agric For Res 66:1–10. https://doi.org/10.3220/LBF1457686750000

[27] Han G, Kawai S, Umemura K, Zhang M, Honda T (2001) Development of high-performance UF-bonded reed and wheat straw medium-density fiberboard. J Wood Sci 47:350–355. https://doi.org/10.1007/BF00766784

[28] Han G, Umemura K, Kawai S, Kajita H (1999) Improvement mechanism of bondability in UF-bonded reed and wheat straw boards by silane coupling agent and extraction treatments. J Wood Sci 45:299–305. https://doi.org/10.1007/BF00833494

[29] Xiao L, Ding Y, Yan G (2021) Effect of hot-pressing temperature on characteristics of alkali pretreated reed straw bio-board. J Wood Chem Technol 41:160–168. https://doi.org/10.1080/02773813.2021.1949351

[30] Ortega Z, Bolaji I, Suárez L, Cunningham E (2023) A review of the use of giant reed (*Arundo donax* L.) in the biorefineries context. Rev Chem Eng. https://doi.org/10.1515/revce-2022-0069

[31] Keijsers E, van den Oever M, Dam JV, Lansbergen A, Koning C, van den Akker H (2020) The development of reed composite fiber boards using partially bio-based, formaldehyde- and monomeric isocyanate-free resins. Reinf Plast 64:195–203. https://doi.org/10.1016/j.repl.2019.10.007

[32] Kraiem D, Pimbert S, Ayadi A, Bradai C (2013) Effect of low content reed (*Phragmite australis*) fibers on the mechanical properties of recycled HDPE composites. Compos B Eng 44:368–374. https://doi.org/10.1016/j.compositesb.2012.04.062

[33] Suárez L, Ortega Z, Barczewski M, Cunningham E (2023) Use of giant reed (*Arundo donax* L.) for polymer composites obtaining: a mapping review. Cellulose 30:4793–4812. https://doi.org/10.1007/s10570-023-05176-x

[34] Shon C-S, Mukashev T, Lee D, Zhang D, Kim JR (2019) Can common reed fiber become an effective construction material? Physical, mechanical, and thermal properties of mortar mixture containing common reed fiber. Sustainability 11:903. https://doi.org/10.3390/su11030903

[35] Jiménez-Espada M, Herrero-Adán D, González-Escobar R (2021) Characterization of mechanical and hygroscopic properties of individual canes of reed. Materials 14:2193. https://doi.org/10.3390/ma14092193

[36] Ghaffar SH, Fan M, McVicar B (2017) Interfacial properties with bonding and failure mechanisms of wheat straw node and internode. Compos A Appl Sci Manuf 99:102–112. https://doi.org/10.1016/j.compositesa.2017.04.005

[37] Obersriebnig M, Konnerth J, Gindl-Altmutter W (2013) Evaluating fundamental position-dependent differences in wood cell wall adhesion using nanoindentation. Int J Adhesion Adhesives 40:129–134. https://doi.org/10.1016/j.ijadhadh.2012.08.011

[38] Ghaffar SH, Fan M (2015) Differential behaviour of nodes and internodes of wheat straw with various pre-treatments. Biomass Bioenergy 83:373–382. https://doi.org/10.1016/j.biombioe.2015.10.020

[39] Jakob M, Mahendran AR, Gindl-Altmutter W, Bliem P, Konnerth J, Müller U, Veigel S (2022) The strength and stiffness of oriented wood and cellulose-fibre materials: a review. Prog Mater Sci 125:100916. https://doi.org/10.1016/j.pmatsci.2021.100916

[40] Reiterer A, Lichtenegger H, Tschegg S, Fratzl P (1999) Experimental evidence for a mechanical function of the cellulose microfibril angle in wood cell walls. Philos Mag A 79:2173–2184. https://doi.org/10.1080/01418619908210415

[41] Nishiyama Y, Langan P, Chanzy H (2002) Crystal structure and hydrogen-bonding system in cellulose Iβ from synchrotron X-ray and neutron fiber diffraction. JACS 124:9074–9082. https://doi.org/10.1021/ja0257319

[42] Alexander GB, Heston WM, Iler RK (1954) The solubility of amorphous silica in water. J Phys Chem 58:453–455. https://doi.org/10.1021/j150516a002

[43] Joščák T, Teischinger A, Müller U, Mauritz R (2006) Production and material performance of long—strand wood composites. Wood Res 51:37–50